RECENT B PHYSICS RESULTS FROM CLEO II

Karen Lingel
(representing the CLEO Collaboration*)
University of Colorado
U.S.A.

ABSTRACT

The large data set collected by the CLEO II detector during 1990-1991 gives us sensitivity to charmless B decay branching ratios approaching the level of the theoretical predictions. We present preliminary results on these rare B decays arising from hadronic $b \to u$ and $b \to s$ transitions. We also present preliminary results on exclusive and inclusive electromagnetic penguins, $b \to s\gamma$.

*The CLEO Collaboration:
*California Institute of Technology —University of California at San Diego
University of California at Santa Barbara —Carnegie-Mellon University
University of Colorado —Cornell University —University of Florida
Harvard University —Ithaca College —University of Kansas —University of Minnesota
State University of New York at Albany —Ohio State University
University of Oklahoma —Purdue University —University of Rochester
Southern Methodist University —Syracuse University —Vanderbilt University*

1. INTRODUCTION

The CLEO II detector is an all-purpose detector located in the south interaction region of the Cornell Electron Storage Ring (CESR). It is described in detail elsewhere.[1] During the 1990-1991 run, we collected 0.507 fb^{-1} of data at the $\Upsilon(4S)$ resonance, which is just above $B\overline{B}$ threshold, and 0.238 fb^{-1} at energies just below $B\overline{B}$ threshold. The data collected on the resonance contain about 1 million produced B's.

2. RARE HADRONIC DECAYS OF B MESONS

The large data sample taken in the 1990-1991 run has allowed us to search for charmless decay modes of B mesons. We concentrate on the decays $B^\circ \to \pi^+\pi^-$ and $B^\circ \to K^+\pi^-$. (Throughout this paper, charge conjugate states are implied.) The reactions can proceed via a tree diagram with a $b \to u$ transition, (Figure 1) which involves the Cabibbo-Kobayashi-Maskawa matrix element V_{ub}, or via penguin diagrams involving $b \to d$ and $b \to s$ transitions, respectively. Interference between the tree and penguin amplitudes can lead to direct CP violation. In addition, the $\pi^+\pi^-$ final state is a CP eigenstate, which means that this mode can be used in a B factory to determine, via B mixing, one of the CP violation angles in the CKM matrix. The CP violation angle is easiest to measure if the tree diagram dominates as expected. The presence of the penguin diagram only complicates the extraction of this angle. For the $K^+\pi^-$ final state, the penguin amplitude is expected to dominate. Theoretical predictions[2,3] for $B^\circ \to \pi^+\pi^-$ are 1 to 2 $\times 10^{-5}$, (assuming $|V_{ub}/V_{cb}| = 0.1$), while predictions[3,4,5] for $B^\circ \to K^+\pi^-$ range from 1 to 7 $\times 10^{-5}$. The previous best upper limit is 9×10^{-5} for each of these modes.[6]

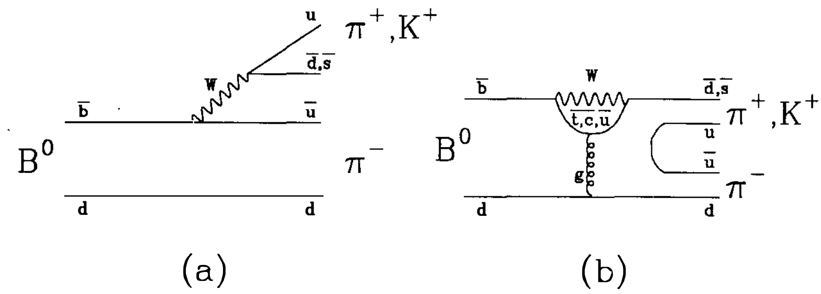

Figure 1: Tree (a) and penguin (b) diagrams for $B^\circ \to \pi^+\pi^-$ and $B^\circ \to K^+\pi^-$.

2.1 Analysis

The analysis is fairly simple. Since the B's are created almost at rest, the two decay products are almost back-to-back, and each has a momentum of about 2.6 GeV. We construct several variables: θ_T, ΔE, and m_B, where θ_T (thrust angle) is the angle between the thrust axis of candidate tracks and the thrust axis of the rest of the tracks plus showers in the event; ΔE (summed daughter energy) $= E_1 + E_2 - E_{\text{beam}}$; and m_B (beam-constrained mass) $= \sqrt{E_{\text{beam}}^2 - (\sum \vec{p_i})^2}$. A cut on thrust angle discriminates against two-jet light quark background; we require $|\cos\theta_T| < 0.7$. ΔE serves two functions: to discriminate against background and also to discriminate between $\pi^+\pi^-$ and $K^+\pi^-$. Our resolution in ΔE is 31 ± 2 MeV; a true $K^+\pi^-$ event reconstructed as $\pi^+\pi^-$ will have (on average) $\Delta E = -42$ MeV, which is 1.3 standard deviations from 0. Note that the beam-constrained mass gives no discrimination between $\pi^+\pi^-$ and $K^+\pi^-$.

2.2 Sorting events into $\pi^+\pi^-$ and $K^+\pi^-$

We use dE/dx for particle identification. At 2.6 GeV momentum, tracks are on the relativistic rise portion of the dE/dx curve, and the separation between kaons and pions is about twice the dE/dx resolution. As noted above, ΔE also provides discrimination between $\pi^+\pi^-$ and $K^+\pi^-$. Therefore, we have used the following χ^2 approach for determining if an event is $\pi^+\pi^-$or $K^+\pi^-$. We construct a χ^2 for each of four hypotheses ($K\pi$, πK, $\pi\pi$, and KK). For the $K\pi$ hypothesis:

$$\chi^2_{K\pi} = \left(\frac{\Delta E_{K\pi}}{\sigma_{\Delta E}}\right)^2 + \left(\frac{\Delta(dE/dx_K)}{\sigma_{dE/dx}}\right)^2 + \left(\frac{\Delta(dE/dx_\pi)}{\sigma_{dE/dx}}\right)^2 \qquad (1)$$

Similar expressions exist for the other hypotheses. Using the χ^2, we can calculate a probability for each hypothesis. We require that the sum of the four probabilities be greater than 10% (to reduce continuum background, in which ΔE is uncorrelated with dE/dx). The event is then sorted into the category with the highest probability. To reduce continuum background, we require $|\Delta E| < 65$ MeV, for the appropriate hypothesis. (The continuum background, which is also composed of kaons and pions, may have very good measurements of dE/dx, allowing unwanted leniency in ΔE.) The resulting beam-constrained mass plots for $\pi^+\pi^-$ and $K^+\pi^-$ are shown in Figure 2. The $\pi^+\pi^-$ channel shows 2 events in the signal region (5.274 to 5.286 GeV), and the $K^+\pi^-$ channel shows 6.

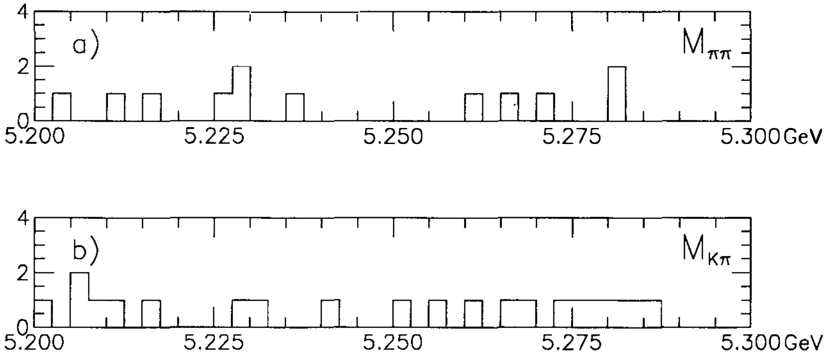

Figure 2: $\pi^+\pi^-$ (a) and $K^+\pi^-$ (b) beam-constrained mass. The signal region (2σ) is 5.274 to 5.286 GeV.

2.3 Background Estimation

We now estimate the background in the signal region. The kinematic momentum limit of tracks from $b \rightarrow c$ decay (including boost) is 2.44 GeV, which is below the energy required by our analysis, thus $b \rightarrow c$ decays cannot be a background. However, $b \rightarrow u$ or $b \rightarrow s$ processes can conceivably be a background if they involve a three-body decay with one massless daughter (such as $B^o \rightarrow \pi^+\ell^-\nu$). Monte Carlo simulations show background from these charmless B decays would be negligible, as expected, since they are rare decays, the massless daughter must be almost at rest, and the charged tracks must be mis-identified. Monte Carlo studies of tau pairs show that tau backgrounds are also negligible.

Thus, we conclude that the background is dominated by continuum production of light quarks. These events will have smooth distributions in ΔE and in beam-constrained mass. We therefore look at a large sideband region in ΔE *vs* mass space surrounding the signal region. The region we select contains about 100 events. We determine the fraction of these events which are $\pi^+\pi^-$, $K^+\pi^-$, and K^+K^-, using a technique similar to the χ^2 method given above, but without using the ΔE term, which is not relevant for background. We then extrapolate into the signal region by using the Monte Carlo to predict the shape of the background. We can double check this background estimation by using conventional methods, namely: a) performing the analysis on the data taken below $B\overline{B}$ threshold, b) using a mass sideband only, and c) using ΔE sidebands only. These methods all give consistent results, and we prefer our two-dimensional sideband method because of the larger statistics. However, for this preliminary analysis, we do not include systematic errors which arise primarily from estimates of the amount of background.

2.4 Preliminary Results

Using the number of observed events, the estimated background, and classical statistics, we calculate preliminary upper limit branching ratios given below:

Table 1: Preliminary upper limit B° branching ratios

mode	eff	N found	est. B	BR UL ($\times 10^{-5}$) 90% CL
$\pi^{+}\pi^{-}$	.31	2	1.2	2.6
$K^{+}\pi^{-}$	.31	6	1.4	5.7

Our upper limit on BR($B^{\circ} \rightarrow \pi^{+}\pi^{-}$) is approaching the theoretical predictions, while our upper limit on BR($B^{\circ} \rightarrow K^{+}\pi^{-}$) is below the Gavela *et al.* prediction, although still above the more recent predictions. We have measured upper limit branching ratios for many other two-body charmless hadronic decays; the upper limits are generally a few 10^{-5}, again approaching the theoretical predictions. The CLEO II data sample has already doubled, and these data will be analyzed soon. In addition, the momentum resolution has been improved, which will lead to better ΔE resolution. We are also working on better methods to discriminate $B\overline{B}$ events from continuum events.

3. ELECTROMAGNETIC PENGUIN DECAY

The charmless decay $B \rightarrow K^{*}\gamma$ can proceed via electromagnetic penguin diagrams such as shown in Figure 3. Since QCD corrections greatly enhance the rate, these processes can give a check of QCD. Theoretical predictions of the inclusive rate are 3 to 4 $\times 10^{-4}$ for $m_{\rm top} \approx 140$ GeV[7]. The Crystal Ball collaboration has determined BR($b \rightarrow s\,\gamma$) < 2.8 $\times 10^{-3}$ (90% CL)[8]. There is large variation in the theoretical estimations for the exclusive modes; predictions for BR($B^{\circ} \rightarrow K^{*\circ}(892)\gamma$) vary from 0.15 to 1.5 $\times 10^{-4}$. The excellent energy resolution and segmentation of the CLEO II CsI calorimeter, as well as the large data set, make it possible to improve these limits.

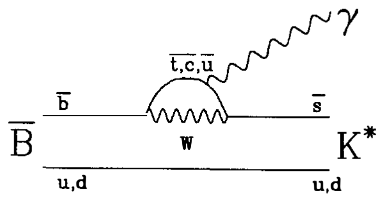

Figure 3: An example of an electromagnetic penguin decay

3.1 Exclusive Two-body Modes

3.1.1 Analysis

In the exclusive analysis, we look for decays of the type $B \to K^*\gamma$ where the K^*'s we look for are listed in Table 2. We look for photons in the barrel region of the calorimeter, $|\cos\theta| < 0.71$, which are unmatched within 20° to a charged track. To ensure that the photon energy is not contaminated with nearby non-associated energy deposit, we require that the ratio of energy in the central nine crystals to that in the twenty-five central crystals must be greater than 0.96. Photons are rejected if they can be paired with a photon (anywhere in the calorimeter) such that $|m_{\gamma\gamma} - m_{\pi^0}| < 14$ MeV or $|m_{\gamma\gamma} - m_\eta| < 28$ MeV. A shower shape requirement (second moment of the shower with respect to its center of mass) reduces the number of candidate photons which are really merged π^0's. Kaon candidate tracks are required to have dE/dx within 2σ of the expected kaon value. K^* candidates' masses are required to be within $\pm 1.5\Gamma$ of the PDG[9] mass. For decay modes involving ρ's, the ρ mass is required to be within $\pm 1.0\Gamma$ of the PDG mass. For decay modes involving π^0's, the π^0 mass must be within 14 MeV (2σ) of the true value. The sum of the energies of the K^* and the γ must be within ± 100 MeV (approximately 2σ) of the beam energy.

To suppress continuum, we make various cuts on event shape. The first is the thrust angle cut explained in section 2.1 above. We require $|\cos\theta_T| < 0.9$. In addition we require that the normalized Fox-Wolfram[10] second moment, $R2$, be less than 0.5. We also require that the sum of the squares of the transverse momenta of all tracks and showers with respect to the γ direction be greater than 1.9 GeV^2. Additional requirements include helicity angle cuts for spin 1 K^*'s, and a B direction cut.

3.1.2 Background Estimation

Background for each mode is estimated by performing the analysis on the data taken at center of mass energy below $B\overline{B}$ threshold, compensating where appropriate for the lower beam energy. The observed number of events in the off-resonance data is scaled by the ratio of the luminosities and corrected for the $1/s$ cross section dependence.

3.1.3 Preliminary Results

Using the number of observed events, the estimated background, and Bayesian statistics, we find the following upper limits:

Table 2: Preliminary upper limits for exclusive $K^*\gamma$ decay modes

Decay mode	K^* decay mode	Eff(%)	BR ($\times 10^{-4}$) (90% C.L.)
$B^0 \to K^{*0}(892)\gamma$	$K^+\pi^-$	18	0.92
$B^+ \to K^{*+}(892)\gamma$	$K^+\pi^0$	5.2	3.7
$B^0 \to K_1^0(1270)\gamma$	$K^+\rho^-$	3.6	5.5
$B^+ \to K_1^+(1270)\gamma$	$K^+\rho^0$	2.9	11
$B^0 \to K_1^0(1400)\gamma$	$K^{*0}(892)\pi^0$, $K^{*+}(892)\pi^-$	8.0	5.4
$B^+ \to K_1^+(1400)\gamma$	$K^{*0}(892)\pi^+$	11	4.8
$B^0 \to K_2^{*0}(1430)\gamma$	$K^+\pi^-$	8.6	1.3
$B^+ \to K_2^{*+}(1430)\gamma$	$K^+\pi^0$	2.2	3.7
$B^0 \to K_3^{*0}(1780)\gamma$	$K^+\rho^-$	3.6	7.6
$B^+ \to K_3^{*+}(1780)\gamma$	$K^+\rho^0$	2.8	14

These upper limit branching ratios for exclusive electromagnetic penguin processes are factors of 2 to 50 times lower than previous measurements. Once again, some of our upper limits are approaching some of the theoretical predictions.

3.2 Inclusive two-body modes

We can search inclusively for two-body electromagnetic penguin decays by looking for an excess of photons above the kinematic limit allowed for photons from $b \to c$ decays. This approach is much less dependent on the details of the hadronization process. However, high energy photons are not an unambiguous signature for the $b \to s\gamma$ process, thus, if a signal is seen, other interpretations (such as $B \to D^*\gamma$) must be ruled out. In addition, one must use a model to determine the fraction of the photons which are in our signal region.

3.2.1 Analysis

We have chosen our signal region to be $2.2 < E_\gamma < 2.7$ GeV. This region takes into account the Doppler energy shift due to the motion of the B, and also covers at least 80% of the photon spectrum from $B \to X\gamma$ for M_X up to nearly 2 GeV.

We have modeled the hadronization process in $b \to s\gamma$ by a spectator model, obtaining estimates of the M_X distribution as well as the photon energy distribution. We take the mass of the s-quark to be the mass of the kaon, and the mass of the spectator quark to be the mass of the pion, thus ensuring that the resulting meson will be above

$K\pi$ threshold. Our model shows that $85 \pm 5\%$ of the resulting photon energy spectrum falls within our signal window. To be conservative we use a lower limit of 70%.

Photons are selected with criteria similar to those in the exclusive analysis. Again, continuum suppression is done using various event shape parameters. We require $R2 < 0.5$. We also define a shape parameter, $S_\perp$, according to the fraction of momentum perpendicular to the photon, $S_\perp = \sum p_\perp / \sum p$ where the numerator includes only tracks which are at least 45° away from the photon. We require $S_\perp > 0.3$. To reduce background coming from initial state radiation, we remove the photon, determine the new center of mass, and make similar event shape cuts in this frame.

3.2.2 Results

Figure 4 shows the photon energy spectrum after (scaled) continuum subtraction.

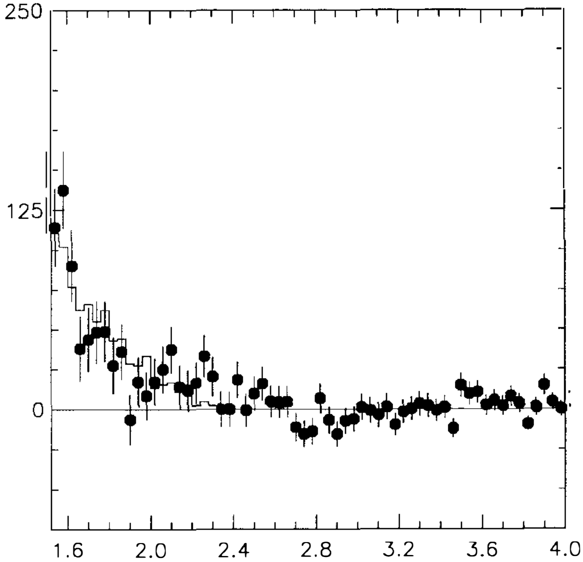

Figure 4: Continuum subtracted photon spectrum. The points are the data, and the solid line is the Monte Carlo for photons arising from $b \to c$ decays. The signal region for $b \to s\gamma$ is 2.2 to 2.7 GeV.

The excess of events at energies below 2.2 GeV is adequately described by our Monte Carlo of photons resulting from $b \to c$ decays. The net number of events above 2.8 GeV (above kinematic limit for B decay) is 18 ± 54, which indicates that our continuum subtraction was done correctly. There is a slight excess of events in the signal energy region: 116 ± 55 events. This gives a preliminary upper limit branching ratio, $BR(b \to s\gamma) < 9.0 \times 10^{-4}$. This is still a factor of 2 larger than most theoretical predictions.

4. CONCLUSIONS

CLEO II has measured new upper limits for rare B decays. The limits for charmless hadronic B decays are a few 10^{-5}, and the limits for electromagnetic penguin modes are a few 10^{-4}. CLEO II is currently running, and expects to have data samples twice as large by the time this is published. Since many of the upper limits presented here are approaching the theoretical predictions, the larger sample promises to yield very exciting results.

ACKNOWLEDGEMENTS

This work is supported by the U.S. Department of Energy and the National Science Foundation.

REFERENCES

1. Y. Kubota *et al.* (CLEO Collaboration) CLNS 91/1122. Submitted to Nucl. Instr. Meth.
2. M. Bauer *et al.*, Z. Phys. C. **34** (1987) 103.
3. L.-L. Chau *et al.*, Phys. Rev. **D43**, (1991) 2176.
4. N. G. Deshpande and J. Trampetic, Phys. Rev. **D41**, (1990) 895.
5. M. B. Gavela *et al.*, Phys. Lett. B **154** (1985) 425.
6. P. Avery *et al.* (CLEO Collaboration), Phys. Lett. B **223** (1989) 470, D. Bortoletto *et al.* (CLEO Collaboration), Phys. Rev. Lett. **62** (1989) 2436.
7. For references on $b \to s\gamma$ and details on this analysis, see P. C. Kim, Proceedings of the Joint International Lepton-Photon Symposium and Europhysics Conference on High Energy Physics, Geneva, 1991, World Scientific Publishing, and references therein.
8. T. Lesiak *et al.* (Crystal Ball Collaboration), DESY-91-075, (1990). Submitted to Z. Phys. C.
9. Particle Data Group, Phys. Lett. B **239**, (1990).
10. G. C. Fox and S. Wolfram, Nucl. Phys. **B149**, (1979) 413.